Methods

Plasmid Constructions. To transform *L. amoebiformis* cells, cDNA fragments of *BnatpD* (AY267652), *Bnfdx1* (AY267628), *BnrpL28* (AY267644), *LaCRT* (FJ209028), *Tgacp* (AF038925), and *Gtlhcp* (AM491789) with artificial restriction sites at both ends were amplified by PCR and inserted between the HindIII and NcoI sites of the pLaRGfp+mc vector generated from the pLaRGfp (32). To introduce mutations (i.e., substitutions or deletions) into the *BnatpD* fragments, we used a PCR-based site-directed mutagenesis technique (40).

To transform *T. gondii* cells, the fragments of *BnatpD* or *Gtlhcp* fused with the *egfp* gene were amplified by PCR, and these fragments were inserted between the EcoRI and PacI sites of the pSAG1/1 CAT vector (41), replacing the CAT gene to generate pSAG-BnAtpD247+GFP and pSAG-GtLhcp233+GFP, respectively. A chimera fragment of *Tgacp* fused with the DsRed-Express gene (Clontech) was generated using the splicing by overlapped extension by PCR (42); it was then inserted into the pSAG1/1 CAT, replacing CAT gene. The resulting fragment, which contained the SAG1 promoter, *Tgacp* fused with *DsRed*, and the SAG1 terminator, was ligated into the SacII site of pTub5CATSag1 vector. All constructs were subsequently sequenced to ensure correct construction.

Transient Transformation. *L. amoebiformis* (CCMP2058) (43) was grown at 20 °C, under white illumination (80–100 μmol photons·m^{-2}·s^{-1}) with a 12-h light/12-h dark cycle, in 500 mL Erlenmeyer flasks containing 300 mL of ESM medium (44). *L. amoebiformis* cells were transformed with plasmid vectors using the Biolistic PDS-1000/He Particle Delivery System (Bio-Rad), as previously described (32). *T. gondii* (RH strain) was maintained by growth in a monolayer of Vero cells in RPMI1640 medium with 3% FCS at 37 °C. The transformation of *T. gondii* was carried out via an electroporation method, using a Gene Pulser Xcell (Bio-Rad) (45). After transformation, those cells were incubated under the conditions described above.

Observation of GFP Localizations. Twenty-four to 48 h after transformation, the transient transformed cells expressing reporter genes were observed under an inverted Zeiss LSM 510 laser scanning microscope (Carl Zeiss); confocal imaging was performed using the single-track mode. GFP fluorescence was detected with a 505–530 nm band pass filter, and plastid autofluorescence and DsRed fluorescence were detected with 585- and 560-nm-long pass filters, respectively, in the excitation line of a 488 nm argon laser and a 543 nm He/Ne laser. The localization of GFP in the transformed cells was also observed using an immunogold localization method under a transmission electron microscope (*SI Methods*).

ACKNOWLEDGMENTS. We thank Dr. L. David Sibley (Washington University, St. Louis, MO) for the pTub5CATSag1 vector and Dr. Shuhei Ota (Station Biologique de Roscoff, France) for technical help using the electron microscope. This work was supported by the Grant-in-Aid for Scientific Research (KAKENHI) on Priority Area "Comparative Genomics" and by Ministry of Education, Culture, Sport, Science, and Technology of Japan Special Coordination Funds for Promoting Science and Technology.

1. McFadden GI (2001) Primary and secondary endosymbiosis and the origin of plastids. *J Phycol* 37:951–959.
2. Keeling PJ, Archibald JM, Fast NM, Palmer JD (2004) Comment on "The evolution of modern eukaryotic phytoplankton." *Science* 306:2191b.
3. Moreira D, Guyader HL, Philippe H (2000) The origin of red algae and the evolution of chloroplasts. *Nature* 405:69–72.
4. Rodríguez-Ezpeleta N, et al. (2005) Monophyly of primary photosynthetic eukaryotes: Green plants, red algae and glaucophytes. *Curr Biol* 15:1325–1330.
5. Cavalier-Smith T (2000) Membrane heredity and early chloroplast evolution. *Trends Plants Sci* 5:174–182.
6. Martin W, et al. (1998) Gene transfer to the nucleus and the evolution of chloroplasts. *Nature* 393:162–165.
7. Bock R, Timmis JN (2008) Reconstructing evolution: Gene transfer from plastids to the nucleus. *BioEssays* 30:556–566.
8. van Dooren GG, Schwartzbach SD, Osafune T, McFadden GI (2001) Translocation of proteins across the multiple membranes of complex plastids. *Biochim Biophys Acta* 1541:34–53.
9. Ishida K (2005) Protein targeting into plastids: A key to understanding the symbiogenetic acquisitions of plastids. *J Plant Res* 118:237–245.
10. Nassoury N, Morse D (2005) Protein targeting to the chloroplasts of photosynthetic eukaryotes: Getting there is half the fun. *Biochim Biophys Acta* 1743:5–19.
11. Patron NJ, Waller RF (2007) Transit peptide diversity and divergence: A global analysis of plastid targeting signals. *BioEssays* 29:1048–1058.
12. Bruce BD (2001) The paradox of plastid transit peptide: Conservation of function despite divergence in primary structure. *Biochim Biophys Acta* 1541:2–21.
13. Steiner JM, Yusa F, Pompe JA, Löffelhaedt W (2005) Homologous protein import machineries in chloroplasts and cyanelles. *Plant J* 44:646–652.
14. Patron NJ, Waller RF, Archibald JM, Keeling PJ (2005) Complex protein targeting to dinoflagellate plastids. *J Mol Biol* 348:1015–1024.
15. Durnford DG, Gray MW (2006) Analysis of *Euglena gracilis* plastid-targeted proteins reveals different classes of transit sequences. *Eukaryot Cell* 5:2079–2091.
16. Kilian O, Kroth PG (2005) Identification and characterization of a new conserved motif within the presequence of proteins targeted into complex diatom plastids. *Plant J* 41:175–183.
17. Gould SB, et al. (2006) Protein targeting into the complex plastid of cryptophytes. *J Mol Evol* 62:674–681.
18. Gould SB, et al. (2006) Nucleus-to-nucleus gene transfer and protein retargeting into a remnant cytoplasm of cryptophytes and diatoms. *Mol Biol Evol* 23:2413–2422.
19. Gruber A, et al. (2007) Protein targeting into complex diatom plastid: Functional characterisation of a specific targeting motif. *Plant Mol Biol* 64:519–530.
20. Foth BJ, et al. (2003) Dissecting apicoplast targeting in the malaria parasite *Plasmodium falciparum*. *Science* 299:705–708.
21. Tonkin CJ, Roos DS, McFadden GI (2006) N-terminal positively charged amino acids, but not their exact position, are important for apicoplast transit peptide fidelity in *Toxoplasma gondii*. *Mol Biochem Parasitol* 150:192–200.
22. Tonkin CJ, et al. (2008) Evolution of malaria parasite plastid targeting sequences. *Proc Natl Acad Sci USA* 105:4781–4785.
23. Ishida K, Green BR, Cavalier-Smith T (1999) Diversification of a chimaeric algal group, the chlorarachniophytes: Phylogeny of nuclear and nucleomorph small-subunit rRNA genes. *Mol Biol Evol* 16:321–331.
24. Rogers MB, Gilson PR, Su V, McFadden GI, Keeling PJ (2007) The complete chloroplast genome of the chlorarachniophyte *Bigelowiella natans*: Evidence for independent origin of chlorarachniophyte and euglenid secondary endosymbionts. *Mol Biol Evol* 24:54–62.
25. McFadden GI, Gilson PR, Hofmann CJB, Adcock GJ, Maier UG (1994) Evidence that an amoeba acquired a chloroplast by retaining part of an engulfed eukaryotic alga. *Proc Natl Acad Sci USA* 91:3690–3694.
26. Gilson PR, et al. (2006) Complete nucleotide sequence of the chlorarachniophyte nucleomorph: Nature's smallest nucleus. *Proc Natl Acad Sci USA* 103:9566–9571.
27. Rogers MB, et al. (2004) Plastid-targeting peptide from the chlorarachniophyte *Bigelowiella natans*. *J Eukaryot Microbiol* 51:529–535.
28. Gile GH, Keeling PJ (2008) Nucleus-encoded periplastid-targeted EFL in chlorarachniophytes. *Mol Biol Evol* 25:1967–1977.
29. Archibald JM, Rogers MB, Toop M, Ishida K, Keeling PJ (2003) Lateral gene transfer and the evolution of plastid-targeted proteins in the secondary plastid-containing alga *Bigelowiella natans*. *Proc Natl Acad Sci USA* 100:7678–7683.
30. Nielsen H, Engelbrecht J, Brunak S, von Heijne G (1997) Identification of prokaryotic and eukaryotic signal peptides and prediction of their cleavage sites. *Protein Eng* 10:1–6.
31. Emanuelsson O, Nielsen H, von Heijne G (1999) ChloroP, a neural network-based method for predicting chloroplast transit peptides and their cleavage sites. *Protein Sci* 8:978–984.
32. Hirakawa Y, Kofuji R, Ishida K (2008) Transient transformation of a chlorarachniophyte alga, *Lotharella amoebiformis* (Chlorarachniophyceae), with *uidA* and *egfp* reporter genes. *J Phycol* 44:814–820.
33. Apt KE, et al. (2002) In vivo characterization of diatom multipartite plastid targeting signals. *J Cell Sci* 115:4061–4069.
34. Rigoutsos I, Floratos A (1998) Combinatorial pattern discovery in biological sequences: The TEIRESIAS algorithm. *Bioinformatics* 14:55–67.
35. Bolte K, et al. (2009) Protein targeting into secondary plastids. *J Eukaryot Microbiol* 56:9–15.
36. Tonkin CJ, Struck NS, Mullin KA, Stimmler LM, McFadden GI (2006) Evidence for Golgi-independent transport from the early secretory pathway to the plastid in malaria parasites. *Mol Microbiol* 61:614–630.
37. Jarvis P, Robinson C (2004) Mechanisms of protein import and routing in chloroplasts. *Curr Biol* 14:R1064–R1077.
38. Cavalier-Smith T (1999) Principle of protein and lipid targeting in secondary symbiogenesis: Euglenoid, dinoflagellate, and sporozoan plastid origins and the eukaryote family tree. *J Eukaryot Microbiol* 46:347–366.
39. Sommer MS, et al. (2007) Der1-mediated preprotein import into the periplastid compartment of chromalveolates? *Mol Biol Evol* 24:918–928.
40. Higuchi R, Krummel B, Saiki RK (1988) A general method of *in vitro* preparation and specific mutagenesis of DNA fragments: Study of protein and DNA interaction. *Nucleic Acids Res* 16:7351–7367.
41. Soldati D, Boothroyd JC (1993) Transient transfection and expression in the obligate intercellular parasite *Toxoplasma gondii*. *Science* 260:349–352.
42. Horton RM, Hunt HD, Ho SN, Pullen JK, Pease LR (1989) Engineering hybrid genes without the use of restriction enzymes: Gene splicing by overlap extension. *Gene* 77:61–68.
43. Ishida K, Ishida N, Hara Y (2000) Lotharella amoeboformis sp nov: A new species of chlorarachniophytes from Japan. *Phycol Res* 48:221–229.
44. Kasai F, Kawachi M, Erata M, Watanabe MM (2004) *NIES-Collection List of Strains: Microalgae and Protozoa* (Microbial Culture Collection, National Institute for Environmental Studies, Tsukuba, Japan), 7th Ed, p 54.
45. Karsten V, Qi H, Beckers CJ, Joiner K (1997) Targeting the secretory pathway of *Toxoplasma gondii*. *Methods* 13:103–111.

植物としてのトキソプラズマ原虫

植物ホルモンとカルシウムシグナリング

Toxoplasma gondii as a plant：Plant hormone and calcium signaling

永宗喜三郎

トキソプラズマ原虫は，植物ホルモンの一種であるアブシジン酸を使って互いに「コミュニケーション」を行い，宿主細胞内で増殖した後の脱出のタイミングを決めていた．アブシジン酸濃度の上昇は，原虫細胞質内カルシウム濃度の上昇をひき起こし，その結果，宿主からの脱出のためのさまざまなイベントが開始されていた．アブシジン酸生合成を阻害すると，原虫はシストへと分化していくことも示された．トキソプラズマ原虫においてこの植物ホルモン産生能は，紅藻が原虫内に共生することにより獲得された細胞内小器官に由来するものと思われた．

Key words ●トキソプラズマ原虫 ●アブシジン酸 ●アピコプラスト ●色素体 ●進化

はじめに

トキソプラズマ原虫はほとんどの温血動物のすべての有核細胞に感染能をもち，全人類の1/3以上，日本人の約25～30％が感染しているといわれている非常に広く蔓延している寄生性原生生物である[1]．多くの感染者にとって，トキソプラズマ感染は不顕性に経過するが，一方でトキソプラズマ感染症は一度発症すると非常に重篤な感染症となる．1999年CDC（米国疾病予防管理センター）からの報告の中では，トキソプラズマ症は，食品由来の感染症による全入院患者のうち原因の明らかになったものの4.1％（第4位），死者数においては20.7％（第3位）にもなると推定されている[2]．また，トキソプラズマ原虫はHIV感染者に致死的な脳炎をひき起こして患者を死に至らしめることが知られており，アメリカでの統計によるとHIV感染患者の18～25％がトキソプラズマ脳炎を発症することが報告されている[3]．一方1999年WHOからの報告によると[4]，1998年の全世界の総死者数の25％を占める感染症による死者のうち，17.3％がAIDSを原因として亡くなっていることと合わせて考えると，世界中の感染症による死者の約4％はトキソプラズマ感染症が原因で亡くなっていると見積もることができる．

トキソプラズマ原虫がヒトに感染した場合，その増殖はタキゾイトとブラディゾイトという2つのステージに分けることができる（図1）．タキゾイトは宿主細胞内に形成された小胞内で急速に増殖するステージで，宿主細胞内への侵入，分裂，宿主細胞からの脱出と次の宿主細胞への移動と付着を次々と繰り返し，感染を広げていく．一方，ブラディゾイト，あるいはシストとよばれるステージでの原虫の分裂は非常に緩慢で，おもに中枢神経系や筋肉系に存在している．シストとなった原虫は宿主の免疫応答から逃れ，宿主が免疫抑制状態になり再活性化できるまで長期間生存する．再活性化した原虫はふたたびタキゾイトとなり感染を再拡大し，宿主の組織を破壊する．

トキソプラズマ原虫が属する，アピコンプレクス門に属する原虫には現在5,000種以上が知られており，すべてが寄生性の原生動物である[5]．このなかにはマラリア原虫やトキソプラズマ原虫，クリプトスポリジウム原虫など人類にとって大きな脅威となっている感染症が含まれている[2,4]．これらアピコンプレクス門に属する原虫の大きな特徴の一つとして，アピコプラストとよばれるオルガネラの存在が挙げられる．アピコプラストは葉緑体が退化してできた四重膜構造の細胞内小器官であり，通常の葉緑体は光合成細菌が植物の祖先に取り込まれて進化したものとされているが，アピコプラストは光合成細菌を取り込んだ紅藻類の祖先が原虫の祖先生物に取り込まれることによって成立したと考えられている[6]（図2）．その

Kisaburo Nagamune
筑波大学大学院・生命環境科学研究科・若手イニシアティブ，現 国立感染症研究所寄生動物部
E-mail：nagamune@nih.go.jp
URL：http://web.me.com/nagamune

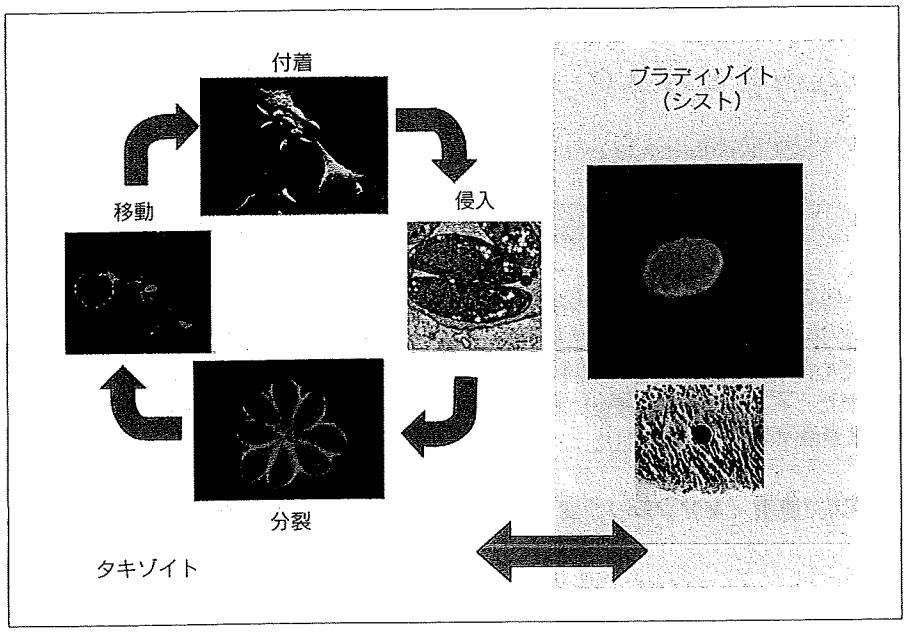

図1　トキソプラズマ原虫の増殖サイクル

ヒトに感染したトキソプラズマ原虫は活発な増殖ステージであるタキゾイトか，あるいは緩慢な増殖ステージであるブラディゾイト(シスト)かのいずれかのかたちで寄生している．タキゾイトのステージにある原虫は，宿主細胞への付着，侵入，宿主細胞内での分裂，宿主細胞を破壊して脱出，次の細胞への移動，というサイクルを繰り返し，活発に増殖を続ける．一方で，ブラディゾイトのステージにある原虫は増殖がほとんど停止し，宿主からの免疫応答から逃れるため被嚢し，再活性化の機会を待つ．

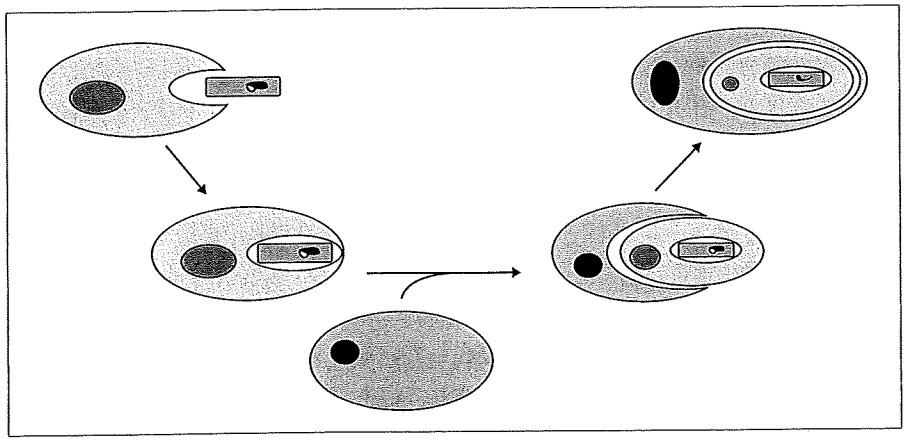

図2　アピコプラストの成立機序

通常の葉緑体は光合成細菌（緑）が植物の祖先（青）に取り込まれて進化したものとされているが，アピコプラストは光合成細菌を取り込んだ紅藻類の祖先が原虫の祖先生物（赤）に取り込まれることによって成立したと考えられている．そのために，アピコプラストは独特の四重膜構造をとる．

ために，アピコプラストは独特の四重膜構造をとる．現在ではアピコプラストは光合成能を失ったものの，脂肪酸合成などの機能を今でも担っており，したがって原虫にとって必須のオルガネラである[7]．しかしながらその機能の詳細は不明であり，なぜ原虫の生存に必須なのかもはっきりとはわかっていない．いずれにしても，アピコンプレクス門原虫の細胞内には植物が「組み込まれている」ということは今やよく知られた事実となっている．最近，筆者らは，トキソプラズマ原虫が植物ホルモンの一種であるアブシジン酸を産生しており，それがトキソプラズマ原虫の細胞質内カルシウム濃度調節をつかさどっていることを明らかにした[8]．本稿では，トキソプラズマ原虫における細胞質内カルシウム濃度調節機構と，植物ホルモンであるアブシジン酸の原虫における意義について考察したい．

I トキソプラズマ原虫の運動・分泌とカルシウムシグナリング

トキソプラズマ原虫は，鞭毛や繊毛のような移動のための特別な器官をもたない．そのため原虫の宿主細胞への侵入は，いわゆる「グライディング」とよばれる原虫アクチン依存的な運動により行われていることが知られている[9]．その際，原虫はマイクロネームとよばれる分泌器官から多数の付着分子を分泌することにより，宿主細胞への付着・侵入が可能となる．このマイクロネーム蛋白質が分泌されるには，原虫の細胞質内カルシウム濃度の上昇が必要である[10]．また，原虫が宿主細胞から脱出す

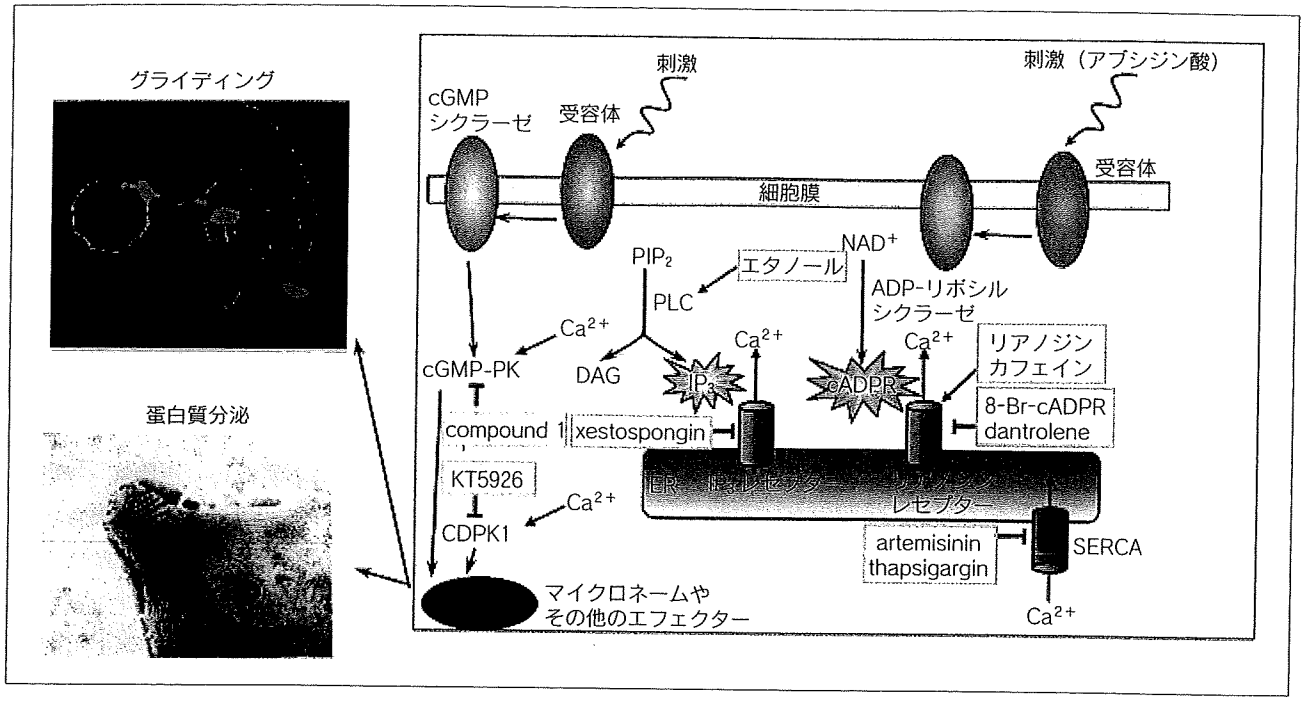

図 3　トキソプラズマ原虫のカルシウムシグナル伝達機構

トキソプラズマ原虫細胞質内カルシウム濃度の上昇は原虫のマイクロネームからの蛋白質分泌や原虫のグライディングを活性化する[13,24,25]．細胞内カルシウム・プールからのカルシウム放出には，cADPR 産生依存的な経路[13]と，IP_3 産生依存的な経路の 2 つがあることが知られている[26]．前者の経路はリアノジンやカフェインにより活性化し，8-Br-cADPR や dantrolene により阻害され，後者の経路はエタノールにより活性化し，xestospongin によって阻害される．カルシウムの再取込みは SERCA によって行われ，thapsigargin や抗マラリア薬である artemisinin は SERCA による細胞質内カルシウムの取込みを阻害していると考えられている[27,28]．細胞質内カルシウム濃度が上昇した後，calcium-dependent protein kinase 1(CDPK1)および cGMP-dependent protein kinase(cGMP-PK)の 2 種類のキナーゼがマイクロネーム蛋白質の分泌に必要であることが報告されている[29,30]．これらのキナーゼはそれぞれ KT5926 および compound 1 により阻害される．これら一連のシグナルを活性化する刺激としては，アブシジン酸が cADPR 依存的なカルシウム放出経路を活性化することが明らかとなった．アブシジン酸および他の刺激に対するレセプターはいまだ明らかになっていない．

るタイミングも細胞質内カルシウム濃度によって調節されることが知られている[11]．薬理学的な解析により，トキソプラズマ原虫は他の生物同様に IP_3 レセプターやリアノジンレセプターを細胞内カルシウム・プールからのカルシウム放出に用いていることが示されてきた．しかしながら，トキソプラズマ原虫に限らず，すべてのアピコンプレクス門原虫のゲノムデータベースからは，ヒトやマウスなどの動物で知られているこれらのレセプターのオルソログ遺伝子は見つからなかった．そこで筆者らはアピコンプレクス門に属する，トキソプラズマ，マラリア，およびクリプトスポリジウム原虫のゲノムデータベースから既知のすべてのカルシウム濃度調節分子遺伝子の同定を試みた[12]．その結果，これらの原虫のカルシウム濃度調節機構は多くの動物のものとは異なり，むしろ，植物的であることを明らかにできた．たとえば，アピコンプレクス門原虫は通常の IP_3 レセプター遺伝子をもっておらず，今まで植物のみで報告されている two-pore calcium

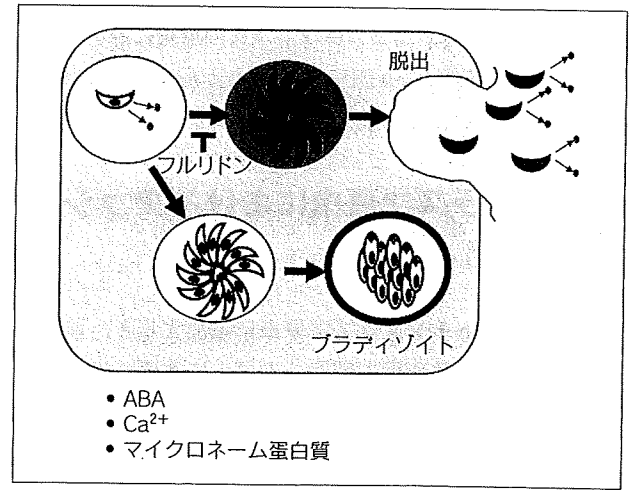

図 4　植物ホルモンであるアブシジン酸がトキソプラズマ原虫に及ぼす影響

アブシジン酸（ピンクの丸）の蓄積が原虫細胞質内カルシウム（青）濃度の上昇をひき起こし，原虫は宿主細胞からの脱出やマイクロネーム蛋白質（緑の丸）の分泌を開始する．フルリドンはアブシジン酸の生合成を阻害し，原虫の脱出を抑制してブラディゾイトへの分化を促進させる．

channel（TPC）遺伝子の存在が見出された．また，同様にこれらの原虫には，植物のみに認められ動物には存在しないとされる，calcium-dependent protein kinase（CDPK）遺伝子が多数認められた．

一方で，動物，植物ともにリアノジンレセプターを介した細胞質内へのカルシウム放出には，サイクリックADPリボース（cADPR）がセカンドメッセンジャーとして広く使われていることが知られている．トキソプラズマ原虫においても，筆者らは，cADPRがセカンドメッセンジャーとして細胞質内カルシウム濃度の上昇をひき起こすことを証明した[13]．また，筆者らは原虫のcADPR合成活性および分解活性を生化学的に証明し，cADPRのアンタゴニストである8-Br-cADPRやdantroleneはトキソプラズマ原虫において，マイクロネーム蛋白質の分泌および原虫のグライディングを阻害することを明らかにした．図3に筆者らや他のグループによって今までに明らかになったトキソプラズマ原虫のカルシウムシグナルの概略を示した．

植物においては，cADPRは植物ホルモンの一種であるアブシジン酸によって産生が誘導され，cADPR産生は植物においても細胞質内カルシウム濃度の上昇をひき起こすことが知られている．またアブシジン酸は，ヒドラや海綿においてもcADPR産生を介した細胞質内カルシウム濃度の上昇をひき起こすことが観察されている[14,15]．また最近，ヒト顆粒球においてもアブシジン酸によるcADPR依存的な細胞質内カルシウム濃度の上昇活性が報告された[16]．これらの事実は，アピコンプレクス門原虫においてもアブシジン酸依存的なcADPRを介したカルシウム放出経路が存在する可能性を示唆しうる．

II トキソプラズマ原虫におけるアブシジン酸

アブシジン酸をトキソプラズマ原虫に添加すると，前述のとおり原虫の運動や宿主細胞への侵入に重要な役割をもつマイクロネーム蛋白質の分泌が誘導された．また筆者らはすでに，マイクロネーム蛋白質の分泌はcADPR依存的な原虫細胞質内カルシウム濃度の上昇に依存していることを見出していたので，実際にアブシジン酸添加後に原虫の産生するcADPRを測定したところ，加えたアブシジン酸量に依存して有意に上昇していた．また，このアブシジン酸によるマイクロネーム蛋白質分泌は細胞質内カルシウム濃度の上昇に依存していることが確認できた．さらにこの活性は天然型のアブシジン酸にのみ存在し，その光学異性体やβ-カロテン，また，レチノイン酸には存在しなかった．

さらに筆者らはELISAやMS解析により，トキソプラズマ原虫が実際にアブシジン酸を産生していることを証明した．アブシジン酸濃度は原虫が宿主細胞から脱出する直前に急激に上昇していた．MS/MS解析により，トキソプラズマ原虫はトランス型およびシス型の両方のアブシジン酸を産生していることが示された．原虫の培養中にアブシジン酸は0.1～0.2μM（通常期）から～4μM（脱出直前）存在していた．これらの値はヒト顆粒球で報告された値の40倍にもなることから，原虫は環境中からアブシジン酸を取り込んでいるのではなく，自らが産生していると考えられる．宿主細胞内の原虫に，外部からアブシジン酸を加えると，原虫の宿主細胞からの脱出が誘導された．また，植物においてアブシジン酸生合成の特異的阻害剤であることが知られているフルリドンは，トキソプラズマ原虫においてもアブシジン酸産生を阻害した．そこで原虫の培養をフルリドン処理すると，トキソプラズマ原虫は加えたフルリドンの濃度依存的に宿主細胞からの脱出が阻害された．しかしながらこの阻害は外部からのアブシジン酸添加によって相補できた．これらのことからアブシジン酸は原虫にとって，宿主細胞からの脱出のシグナルになっている可能性が考えられた．以上の結果から，トキソプラズマ原虫はアブシジン酸を産生しており，アブシジン酸は原虫内でカルシウム放出のセカンドメッセンジャーであるcADPR産生を誘導し，細胞質内カルシウム濃度を上昇させ，宿主細胞からの脱出やそれに伴うグライディングと次の宿主細胞への侵入を促進するという一連のシグナルの存在が示唆された（図4）．

また，アブシジン酸生合成阻害剤フルリドンの培養中への添加によってアブシジン酸の生合成を阻害すると，原虫のブラディゾイトへの分化が誘導された（図1, 4）．高等植物において，アブシジン酸は種子の休眠状態を維持したり，発芽を抑制したりすることにより，発育を抑制的にコントロールしていることが知られている[17]．また高等植物においては，浸透圧，低温，塩などによるストレスによりアブシジン酸生合成遺伝子の発現レベルが上昇することも報告されている[17]．したがってアブシジン酸は植物にとって一種の「抗ストレスホルモン」として，

ストレス条件に対する耐性の上昇にはたらいていると考えることもできる．トキソプラズマ原虫においてはアブシジン酸の濃度の減少がブラディゾイトへの分化，すなわち休眠状態への移行を誘導したことから，植物で知られている抗ストレス反応とは，一見逆に見える作用を示した．トキソプラズマ原虫にとって通常，ブラディゾイトによる休眠は，栄養の不足や種々のストレスによってひき起こされるストレス応答の一種であると考えられている[18]ので，トキソプラズマ原虫においてもアブシジン酸が「抗ストレスホルモン」としてはたらいているのであれば，フルリドンによるアブシジン酸生合成の減少は，原虫を環境中のストレスへの耐性を減少させる方向にはたらき，それによって高濃度のアブシジン酸存在下で抑制されていた分化へのパスウエィが動き始めるのかもしれない．

フルリドンは一方で，マウスを用いたトキソプラズマ感染実験において，マウスの致死率を有意に減少させた．このことは，アブシジン酸生合成の阻害が原虫の宿主細胞からの脱出を抑制することによる感染拡散の阻止の結果であると推定できた．この結果はフルリドンが哺乳動物に対し毒性が弱く，除草剤として用いられている事実と合わせて考えると，フルリドン，あるいはアブシジン酸生合成阻害剤は抗トキソプラズマ薬開発のよいリード化合物となる可能性が示唆される．

おわりに

マラリアやトキソプラズマ原虫をはじめとする，多くのアピコンプレクス門原虫はアピコプラストとよばれる紅藻由来の共生器官をもっていることから，これらアピコンプレクス門原虫は葉緑体由来の多くの代謝経路をいまだ保持している可能性が考えられている．事実，アピコンプレクス門原虫はイソプレノイドを合成するための経路（メバロチン経路）を消失しており，そのためイソプレノイド合成は，アピコプラストに存在している植物と同じDOXP-MEP経路に依存していることが知られている[9]．高等植物において，アブシジン酸の生合成の多くは葉緑体内で行われていることと，アブシジン酸生合成はイソプレノイドからβ-カロテンを合成することにより開始されることから[19]，おそらくトキソプラズマ原虫においてもアブシジン酸生合成の大部分はアピコプラストにおいて行われている可能性が示唆できる．また，アピコンプレクス門原虫においてすでに光合成能を失ったアピコプラストがいまだ原虫の生存に必須であるという理由の一つに，今回見出されたアブシジン酸生合成経路の存在があるのかもしれない．

筆者らはアブシジン酸生合成遺伝子オルソログ候補遺伝子をトキソプラズマおよびマラリアゲノムデータベースからいくつか同定している．しかしながらこれらの遺伝子は高等植物の遺伝子とのホモロジーが低く，また，既知のすべての遺伝子が同定できたわけでもない．このことは，おそらく，原虫のアブシジン酸生合成経路がアピコプラスト由来，すなわち紅藻由来であるためであると思われる．高等植物においてもアブシジン酸生合成の大部分が葉緑体で行われていることから，アブシジン酸生合成経路が藍藻，あるいは真核藻類に保存されている可能性は低くないものと思われる．実際，緑藻，紅藻，褐藻，さらには原核生物である藍藻類にまでアブシジン酸産生能力があることが報告されている[20~23]．しかしながらこれら藻類のアブシジン酸生合成経路はあまりよくわかっていない．今後各藻類のアブシジン酸生合成経路および生合成にかかわる遺伝子群が明らかとなれば，トキソプラズマ原虫のアブシジン酸生合成経路の起源，つまりアピコンプレクス門原虫におけるアピコプラストの起源が明らかとなり，トキソプラズマ原虫やマラリア原虫の進化の過程を理解することに一つの大きなヒントを得ることができると考えられる．また，同時に効果的な抗原虫薬開発への大きな足がかりになる可能性が期待できる．

文　献

1) Dubey, J. P.：*in* "Toxoplasma gondii", (edited by Weiss, L. M., Kim, K.), pp. 1-17, Academic Press (2007)
2) Mead, P. S. *et al*.：*Emerging Infect. Dis*., 5, 607-625 (1999)
3) Kasper, L. H., Buzoni-Gatel, D.：*Parasitol. Today*, 14, 150-156 (1998)
4) "World Health Organization Report on Infectious Diseases：Removing obstacles to healthy development", WHO (1999)
5) Levine, N. D.："The Protozoan Phylum Apicomplexa", CRC Press (1988)
6) Archibald, J. M., Keeling, P. J.：*Trends Genet*., 18, 577-584 (2002)
7) Ralph, S. A. *et al*.：*Nat. Rev. Microbiol*., 2, 203-216 (2004)
8) Nagamune, K. *et al*.：*Nature*, 451, 207-210 (2008)
9) Sibley, L. D.：*Science*, 304, 248-253 (2004)
10) Lovett, J. L., Sibley, L. D.：*J. Cell Sci*., 116, 3009-3016 (2003)
11) Black, M. W. *et al*.：*Mol. Cell Biol*., 20, 9399-9408 (2000)
12) Nagamune, K., Sibley, L. D.：*Mol. Biol. Evol*., 23, 1613-1627

(2006)
13) Chini, E. N. *et al.* : *Biochem. J.*, 389, 269-277 (2005)
14) Puce, S. *et al.* : *J. Biol. Chem.*, 279, 39783-39788 (2004)
15) Zocchi, E. *et al.* : *Proc. Natl. Acad. Sci. USA*, 98, 14859-14864 (2001)
16) Bruzzone, S. *et al.* : *Proc. Natl. Acad. Sci. USA*, 104, 5759-5764 (2007)
17) Xiong, L., Zhu, J. K. : *Plant Physiol.*, 133, 29-36 (2003)
18) Weiss, L. M., Kim, K. : *in* "Toxoplasma gondii", (edited by Weiss, L. M., Kim, K.), pp. 341-366, Academic Press (2007)
19) Schwartz, S. H. *et al.* : *Plant Phyiol.*, 131, 1591-1601 (2003)
20) Hirsch, R. *et al.* : *Botanica Acta*, 102, 326-334 (1989)
21) Cowan, A. K., Rose, P. D. : *Plant Physiol.*, 97, 798-803 (1991)
22) Marsalek, B. *et al.* : *J. Plant Physiol.*, 139, 506-508 (1992)
23) Kobayashi, M. *et al.* : *Plant Growth Reg.*, 22, 79-85 (1997)
24) Carruthers V. B. *et al.* : *Biochem. J.*, 342, 379-386 (1999)
25) Carruthers V. B. *et al.* : *Cell Microbiol.*, 1, 225-235 (1999)
26) Lovett J. L. *et al.* : *J. Biol. Chem.*, 277, 25870-25876 (2002)
27) Nagamune, K. *et al.* : *Antimicrob. Agents Chemother.*, 51, 3816-3823 (2007)
28) Nagamune, K. *et al.* : *Eukaryotic Cell*, 6, 2147-2156 (2007)
29) Kieschnick, H. *et al.* : *J. Biol. Chem.*, 276, 12369-12377 (2001)
30) Wiersma, H. I. *et al.* : *Int. J. Parasitol.*, 34, 369-380 (2004)

doi: 10.1111/j.1346-8138.2009.00592.00594.x

Journal of Dermatology 2009; **36**: 86–89

CASE REPORT

Case of creeping disease treated with ivermectin

Yuko SENBA,[1] Kenshiro TSUDA,[1] Haruhiko MARUYAMA,[2] Ichiro KUROKAWA,[3] Hitoshi MIZUTANI,[3] Yoshiki TANIGUCHI[1]

[1]*Department of Dermatology, Yokkaichi Municipal Hospital, Mie,* [2]*Division of Parasitology, Department of Infectious Diseases, Faculty of Medicine, University of Miyazaki, Kiyotake, Miyazaki, and* [3]*Department of Dermatology, Mie University Graduate School of Medicine, Mie, Japan*

ABSTRACT

We report a case of creeping disease treated successfully with ivermectin. A 46-year-old man presented with a 1-month history of pruriginous linear erythema on his right thigh after a visit to Indonesia. Although he had no history of eating raw fish or meat, he walked along the river and in the jungle without wearing shoes. Creeping disease caused by animal hookworm was strongly suspected. The presence of parasite larvae was not confirmed in biopsied skin specimens. In enzyme-linked immunosorbent assay, serum samples were negative for binding to hookworm antigens, including Ancylostoma canium, Necator americanus and Gnathostoma doloresi. He was treated with a single 12 mg oral dose (200 μg/kg) of ivermectin. The eruption and pruritus resolved within a few days after the administration and did not relapse.

Key words: ancylostoma, creeping eruption, hookworm, ivermectin, larva migrans.

INTRODUCTION

Creeping disease (cutaneous larva migrans) is a skin disease due to infection by the larval form of nematodes. In Japan, creeping disease caused by Gnathostoma spp. is most common in people who eat freshwater fish or the Japanese copperhead snake, whereas larval hookworm infection such as Ancylosotoma canium and Ancylostoma brasilliense is rare and is usually present as percutaneous infection.[1]

Ivermectin has been commonly used against onchocerciasis and scabies.[2] Recently, some cases have been reported of creeping disease treated successfully by oral administration of ivermectin in European and North American countries.[3–6] However, we are aware of only two patients with Ancylostoma spp. infection treated with ivermectin in Japan.[6,7] Herein, we present a case of creeping disease, probably caused by animal hookworms, successfully treated with ivermectin. We also report the results of microplate enzyme-linked immunosorbent assay (ELISA).

CASE REPORT

A 46-year-old-male Japanese office worker consulted our clinic, complaining of an itchy rash elongating by 1 cm per day on his right posterior thigh. He noticed the eruption after travelling to Indonesia. He denied eating any raw fish or meat, but admitted to walking along a river and in the jungle without shoes, and he had a history of leech bite. Creeping disease was suspected because of the typical clinical manifestation.

Serpiginous linear erythema, 2–3 mm wide, was distributed on the back of his right thigh (Fig. 1a). Pinhead-sized papules and vesicles were found at the edge of the erythema. The patient complained of pruritus. Laboratory examination did not reveal eosinophilia or elevation of immunoglobulin (Ig)E levels.

Three days after his first visit, the fresh linear erythema had elongated by approximately 3 cm (Fig. 1b). Ultrasonography did not show presence of the parasite. Histology showed moderate eosinophilic

Correspondence: Yuko Senba, M.D., Department of Dermatology, Mie University Graduate School of Medicine, 2-174, Edobashi, Tsu, Mie 514-8507 Japan. Email: senba-y@clin.medic.mie-u.ac.jp

Received 17 June 2008; accepted 27 October 2008.

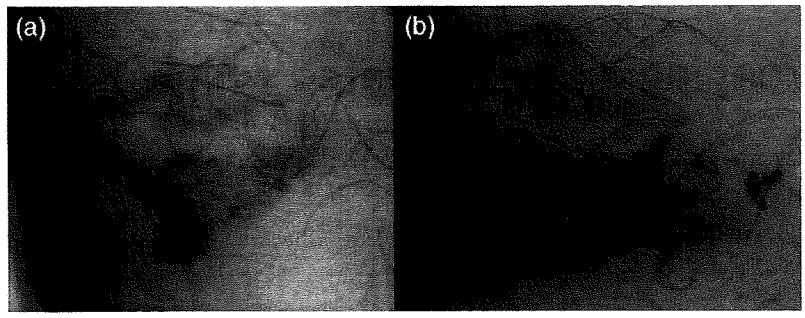

Figure 1. (a) A serpiginous linear erythema on the thigh. (b) A fresh erythema elongating approximately 3 cm long. A skin biopsy was taken from two different locations, indicated by the black arrows.

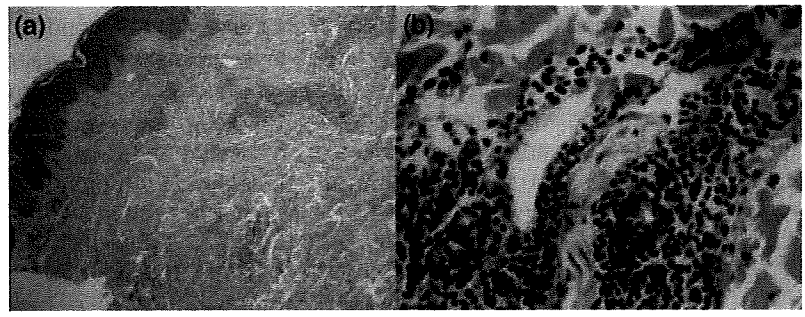

Figure 2. Perivascular eosinophilic infiltration in the dermis is noted. The parasite or the larva tract was not detected (original magnification: [a] ×40; [b] ×400).

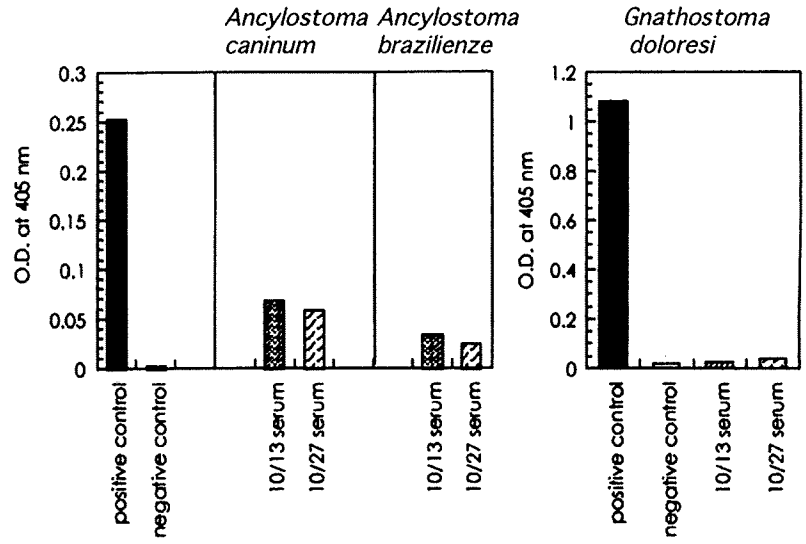

Figure 3. Specific immunoglobulin (Ig)G antibody titers in the sera were measured by microplate enzyme-linked immunosorbent assay using Necator americanus, Ancylostoma caninum and Gnathostoma doloresi. Significant elevation of the titers was not observed. (Positive control was serum from an ancylostomiasis patient in Papua New Guinea. Negative control was sera from healthy volunteers of Miyazaki University.)

infiltration around the small blood vessel. However, neither the body of the parasite nor a cleft indicating the larva tract were detectable (Fig. 2). We investigated the sera from the patient, sampled before and after the treatment. Specific IgG antibody titers in the sera were measured by microplate ELISA using human hookworm (Necator americanus), dog hookworm (Ancylostoma caninum) and Gnathostoma

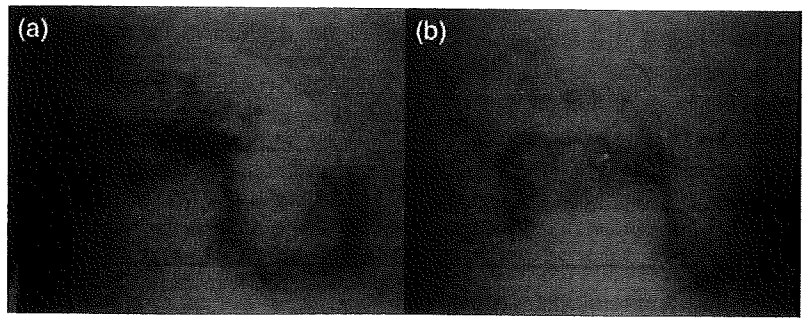

Figure 4. (a) Further elongation of fresh erythema. (b) A brown-colored pigmentation 4 days after taking ivermectin.

(Gnathostoma doloresi) (Fig. 3). Examination for Gnathostoma was negative. Antibody titers against N. americanus and A. caninum were above the negative control, although, compared with the positive control, immunoreactions of the patient's sera were weak. Because the titer was below 0.1 (optical density, 450 nm), we considered that elevation of the titer was not significant.

We diagnosed this case as creeping disease, because of the typical serpiginous erythema and a history of traveling in southeast Asia. Creeping disease caused by percutaneous infection such as A. canium and A. brasilliense was strongly suspected.

One week after the biopsy, further elongation of the worm tunnel was observed (Fig. 4a). A single oral dose of 200 μg/kg ivermectin between meals was then administered. Four days after taking ivermectin, the erythema faded (Fig. 4b). The pruritus resolved within 2 days of the administration. Neither adverse reaction nor recurrence was observed.

DISCUSSION

Creeping disease is an infectious skin disease caused by the larval form of nematodes. Our case was considered as a percutaneous larval hookworm infection. The patient had traveled to southeast Asia, where the main species is A. brasilliense, which is common in tropical areas, but A. canium and other canine species may also be the cause of the pathogen. According to Bouchaud et al.,[3] in cases of creeping disease with Ancylostoma spp., the incubation period is usually not more than 1 month, and pruritus was observed in all cases. The creeping eruption caused by A. brasilliense can resolve spontaneously in most cases, because the larvae are not able to complete their life cycle within humans and die after several months. However, our patient continued to suffer from severe pruritus, and was treated with a single oral dose of 200 μg/kg ivermectin. Previous reports state that the mean interval between ivermectin intake and the disappearance of pruritus is 3 days, and the mean interval between ivermectin therapy and the disappearance of lesions is 9 days.[3]

Ivermectin is a semisynthetic macrolide endectocide which has been often used against onchocerciasis and scabies.[2] Recently, several reports from Europe and North America have reported the efficacy of ivermectin against creeping disease. In a prospective study performed in France, 64 patients with creeping disease were enrolled and treated with a single 200 μg/kg dose of ivermectin taken between meals,[3] and 77% of them were cured. After one or two supplementary doses, the overall cure rate reached 97%. In a previous report by Caumes et al., a single 400 μg/kg dose of ivermectin was effective for all 10 patients.[4] Karavichian et al. reported that 17 patients were treated with a single 200 μg/kg dose of ivermectin, and 76% patients were cured.[5] However, we know of only two cases of creeping disease treated with ivermectin published in Japan.[6,7]

To confirm the diagnosis, it is necessary to detect the larvae in the biopsied specimen. But this is difficult because the parasite moves rapidly beyond the obvious lesion. Therefore, we measured the parasite-specific IgG antibody titers in the patient's sera by microplate ELISA. The elevation of the antibody titers, however, was not significant. Immunoserological examination is known to show negative

in most patients with A. brasilliense and A. canium infection, because hookworms are too small to cause sufficient immunoresponse and produce antibody.[8] According to Uchiyama et al., only three of seven suspected cases of Ancylostomas spp. infection showed seropositive against two hookworm antigens (N. americanus and A. caninum).[1] In contrast, in cases with Gnathostoma and Ascaris spp. infection, microplate ELISA is usually positive and has diagnostic significance.[9] Immunoserological examination may be of limited help in the diagnosis of creeping disease by Ancylostoma spp. and Ascaris spp. because it shows false-negative in many patients.

REFERENCES

1 Nakamura-Uchiyama F, Yamasaki E, Nawa Y. One confirmed and six suspected cases of cutaneous larva migrans caused by overseas infection with dog hookworm larvae. J Dermatol 2002; 29: 104–111.

2 Dourmishev AL, Dourmishev LA, Schwartz RA. Ivermectin: pharmacology and application in dermatology. Int J Dermatol 2005; 44: 981–988.

3 Bouchaud O, Houze S, Schiemann R et al. Cutaneous larva migrans in travelers: a prospective study, with assessment of therapy with ivermectin. Clin Infect Dis 2000; 31: 493–498.

4 Caumes E. Treatment of cutaneous larva migrans. Clin Infet Dis 2000; 30: 811–814.

5 Kravichian K, Nuchprayoon S, Sitichalernchai P, Chaicumpa W, Yentakam S. Treatment of cutaneous gnathostomiasis with ivermectin. Am J Trop Med Hyg 2004; 71(5): 623–628.

6 Kinoshita Y, Hara H, Ochiai T, Suzuki H, Morishima K, Nawa Y. [Creeping eruption caused by the larva of Ancylostoma brasilliense.] Hihukano-rinsyo 2003; 45(2): 125–127. (In Japanese.)

7 Murayama J, Ono H, Taniguchi H, Takino C, Ohtaki N, Akao N. Creeping eruption caused by the hookworm larva. Hihukano-rinsyo 2006; 48(5): 671–673 (in Japanese).

8 Nakamura-Uchiyama F. [Cutaneous larva migrans.] Hihukano-rinsyo 2004; 46(11): 1635–1645. (In Japanese.)

9 Maruyama H, Noda S, Choi WY, Ohta N, Nawa Y. Fine binding specificities to Ascaris suum and Ascaris lumbricoides antigens of the sera from patients of probable visceral larva migrans due to Ascaris suum. Parasitology Int 1997; 46: 181–188.

Circ J 2009; 73: 1344–1348

Fulminant Eosinophilic Myocarditis Associated With Visceral Larva Migrans Caused by Toxocara Canis Infection

Kenki Enko, MD; Takeshi Tada, MD; Keiko O. Ohgo, MD; Satoshi Nagase, MD; Kazufumi Nakamura, MD; Kei Ohta, MD*; Shingo Ichiba, MD*; Yoshihito Ujike, MD*; Yukifumi Nawa, MD**; Haruhiko Maruyama, MD**; Tohru Ohe, MD; Kengo F. Kusano, MD

A 19-year-old man was transferred to hospital because of myocarditis with cardiogenic shock. Echocardiography showed a left ventricular ejection fraction of 23.8% and an intermediate amount of pericardial effusion. The patient immediately received an intra-aortic balloon pump and percutaneous cardiopulmonary support. Right ventricular endomyocardial biopsy was performed in the acute phase and showed extensive eosinophilic inflammatory cell infiltration, severe interstitial edema and moderate myocardial necrosis. High-dose corticosteroids were administered. Because the patient's antibody titer against Toxocara canis was high and his symptoms had appeared after eating raw deer meat, the diagnosis was fulminant eosinophilic myocarditis caused by a hypersensitivity reaction to visceral larval migrans. After starting high-dose corticosteroids, the ejectionfraction dramatically improved, the eosinophilia decreased and the patient made a full recovery. (Circ J 2009; 73: 1344–1348)

Key Words: Corticosteroids; Eosinophilia; Myocarditis; Toxocara canis; Visceral larva migrans

Acute myocarditis occasionally progress to a fulminant course, which can be fatal without mechanical support. Most of these fulminant cases are caused by viral infection for which corticosteroids are not effective[1,2] Visceral larva migrans (VLM), described by Beaver et al in 1952[3] results mainly from infection by the common roundworms of dogs and cats, Toxocara (T.) canis and T. cati, respectively. Infection with the parasite usually causes marked eosinophilia and the development of eosinophilic-rich granulomatous lesions in the soft tissues of the body, including the myocardium[4,5] It has been reported that administration of high-dose corticosteroids in the early stage can dramatically improve eosinophilic myocarditis, but fulminant cases are usually diagnosed at autopsy. We report a rare case of fulminant eosinophilic myocarditis caused by a hypersensitivity reaction to VLM.

Case Report

A 19-year-old man presented at a local hospital complaining of chest discomfort and pain. He had been healthy with no significant preceding symptoms, allergic history or past medical history. ECG showed a slight ST elevation in all limb and precordial leads, except for aVR (Figure 1A). Chest X-ray showed cardiomegaly, pulmonary congestion

Table 1. Results of Blood Examination on Admission

Complete blood count	
WBC	22,900/μl
Neutrophils	72.2%
Lymphocytes	16.6%
Monocytes	6.6%
Eosinophils	4.6% (1,053/μl)
Basophils	0%
RBC	560×10⁴/μl
Hemoglobin	17.9 g/dl
Hematocrit	54.3%
Platelets	25.8×10⁴/μl
Blood chemistry	
Total bilirubin	3.09 mg/dl
Total protein	5.8 g/dl
Albumin	3.6 g/dl
AST	2,462 IU/L
ALT	2,967 IU/L
LDH	2,126 IU/L
CK	144 IU/L
Troponin T (+)	
BUN	24.7 mg/dl
Cr	1.21 mg/dl
UA	10.2 mg/dl
Na	130 mmol/L
K	4.9 mmol/L
Cl	100 mmol/L
CRP	4.0 mg/dl
ECP	54.9 ng/ml
Infection markers	
HBs-Ag	(–)
HCV-AB	(–)
STS	(–)
TPHA	(–)

WBC, white blood cells; RBC, red blood cells; AST, aspartate aminotransferase; ALT, alanine aminotransferase; LDH, lactate dehydrogenase; CK, creatine kinase; BUN, blood urea nitrogen; Cr, creatinine; UA, uric acid; CRP, C-reactive protein; ECP, eosinophil cationic protein; HBs-Ag, hepatitis B surface antigen; HCV, hepatitis C virus; TPHA, Treponema pallidum hemagglutination.

(Received April 4, 2008; revised manuscript received July 17, 2008; accepted July 23, 2008; released online December 27, 2008)

Departments of Cardiovascular Medicine, *Emergency and Critical Care Medicine, Okayama University Graduate School of Medicine, Dentistry, and Pharmaceutical Science, Okayama and **Department of Parasitology, Faculty of Medicine, University of Miyazaki, Miyazaki, Japan

Mailing address: Kengo F. Kusano, MD, Department of Cardiovascular Medicine, Okayama University Graduate School of Medicine, Dentistry, and Pharmaceutical Sciences, 2-5-1 Shikata-cho, Okayama 700-8558, Japan. E-mail: Kfuku0218@aol.com

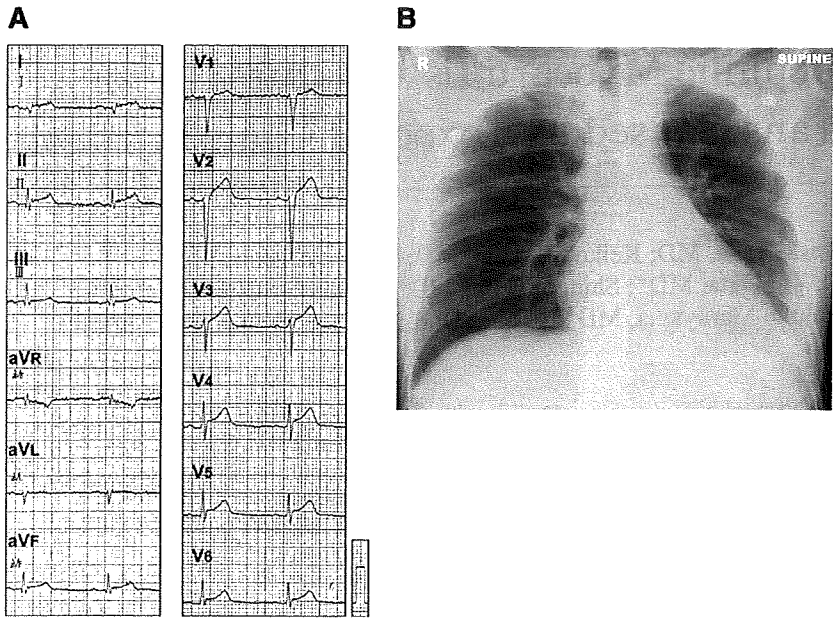

Figure 1. (A) Twelve-lead ECG on admission shows ST elevation. (B) Chest X-ray on admission shows the enlarged cardiac silhouette with pleural effusion.

Table 2. Viral Antibody Tests

Acute phase (admission)	Chronic phase (day 18)
Positive	Positive
Coxsackie virus A16 (×64)	Coxsackie virus A16 (×64)
Coxsackie virus B4 (×32)	Coxsackie virus B4 (×16)
Parainfluenza 3 (×40)	Parainfluenza 3 (×40)
Herpes simplex (×16)	Herpes simplex (×16)
Echo 12 (×32)	Echo 12 (×16)
Negative	Negative
Echo 3, 6, 7, 11	Echo 3, 6, 7, 11
Coxsakie virus A7	Coxsakie virus A7
Coxsakie virus B1, B2, B3, B5, B6	Coxsakie virus B1, B2, B3, B5, B6
Adenovirus, mumps virus, RS virus	Adenovirus, mumps virus, RS virus

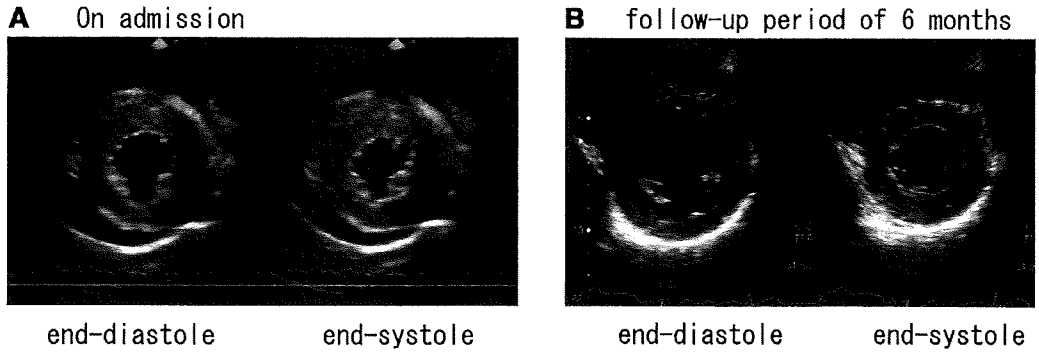

Figure 2. Echocardiography. (A) Large amount of pericardial effusion, wall thickening and severely decreased wall motion. (B) Six months after discharge, all abnormalities have improved dramatically.

and left pleural effusion (Figure 1B). He was admitted as an emergency with the suspicion of acute pericarditis. After admission, his general condition and left ventricular ejection fraction (LVEF) rapidly deteriorated and administration of dopamine was started because of cardiogenic shock. The next day he was transferred to our hospital for treatment of fulminant myo/pericarditis of unknown etiology.

On admission, his systolic blood pressure was 80 mmHg and heart rate was 130 beats/min with paradoxical pulse. A third heart sound was audible and his jugular vein was distended. Hematological and serological examinations (Table 1) showed marked increases in the total white blood cell count (22,900/μl) and eosinophil count (1,053/μl). C-reactive protein was also elevated (4.0 mg/dl), as was eosin-

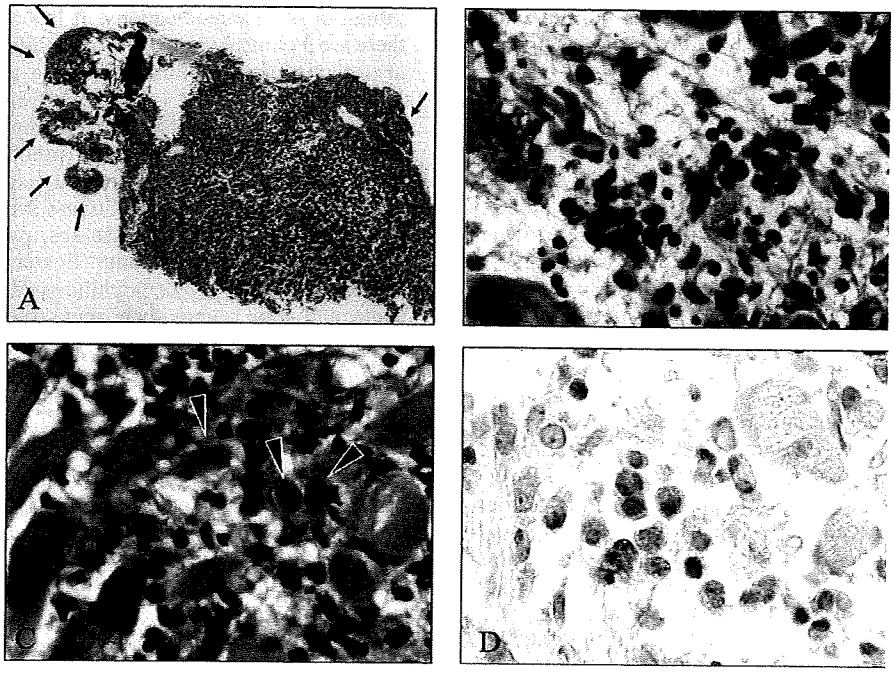

Figure 3. (A) Diffuse inflammatory infiltrate of the myocardium and endocardial involvement by mural thrombi containing eosinophils (arrows; H&E, ×25). (B) Eosinophil-rich inflammatory infiltrate with associated interstitial edema (H&E, ×200). (C) Interstitial Inflammatory infiltrated with associated myocyte necrosis (arrowheads; H&E, ×400). (D) Infiltrating eosinophils revealed by immunostaining with major basic protein (×400).

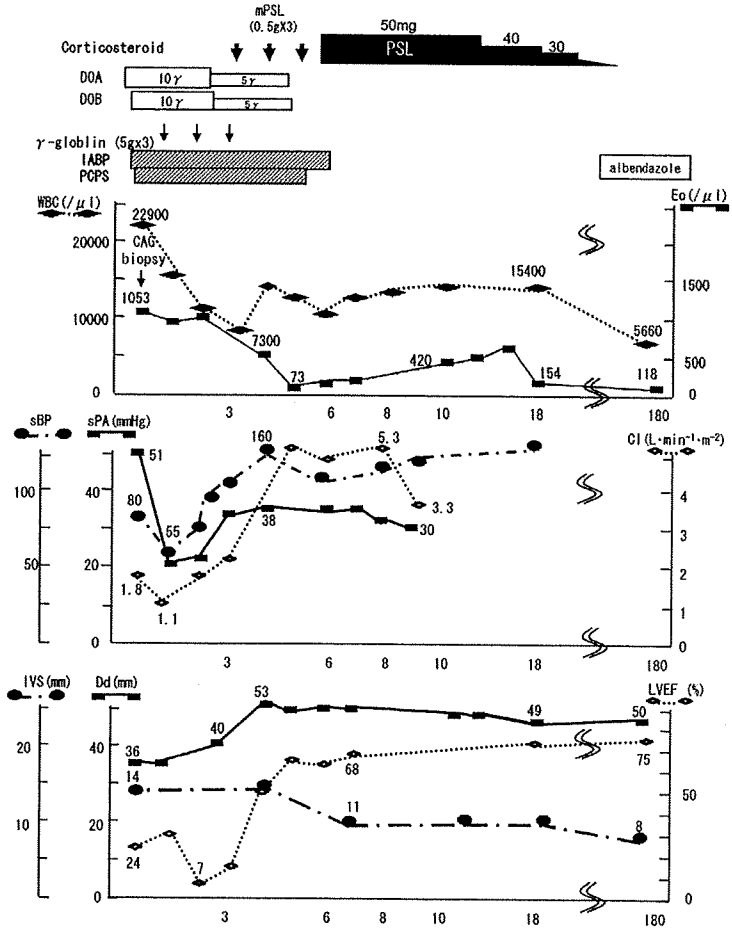

Figure 4. Clinical course. After starting corticosteroid treatment, LVEF and CI dramatically improved, with a decrease in the number of eosinophils. mPSL, methylprednisolone; PSL, prednisolone; DOA, dopamine; DOB, dobutamine; IABP, intra-aortic balloon pump; PCPS, percutaneous cardiopulmonary support; WBC, white blood cell count; Eo, eosinophil; sBP, systolic blood pressure; sPA, systolic pulmonary artery pressure; CI, cardiac index; IVS, interventricular septum; Dd, left ventricular end-diastolic dimension; LVEF, left ventricular ejection fraction.

ophilic cationic protein (ECP: 54.9 ng/ml; normal range: <14.7 ng/ml). Immunological examination on the first day of admission revealed positive antibody titers for Coxsackie virus A16, Coxsackie virus B4, parainfluenza 3, herpes simplex and echo 12 were positive, and negative titers for adenovirus, mumps, Coxsackie virus, echovirus (except for type 12), herpes simplex, parainfluenza, and RS virus. However, there was no significant change in the antibody titers in the tests performed in the chronic phase, which ruled out the active phase of viral infection (Table 2).

Echocardiography showed severe hypokinesis of the left ventricular wall motion (LVEF: 23.8%), with thickening of the left ventricle and a large amount of pericardial effusion (Figure 2A). A diagnosis of fulminant myocarditis with cardiogenic shock was made. An intra-aortic balloon pump (IABP) and percutaneous cardiopulmonary support (PCPS) were immediately inserted and cardiac catheterization was then performed to decide the course of treatment.

Coronary angiography revealed no stenotic lesions. Right heart catheterization showed a pulmonary artery systolic pressure of 51 mmHg, pulmonary artery wedge pressure of 20 mmHg, and right atrial pressure 18 mmHg. Right ventricular endomyocardial biopsy was performed and histopathology revealed extensive interstitial edema with diffuse inflammatory interstitial infiltrate and myocardial necrosis. The infiltrating cells were eosinophils that had partially degranulated. These findings were compatible with acute eosinophilic myocarditis (Figure 3).

We started intravenous methylprednisolone at 500 mg/day for 3 days, followed by oral administration of prednisolone at 50 mg/day. After starting corticosteroid therapy, his ventricular function dramatically improved and the eosinophil count decreased promptly and normalized. On day 6 (day 1 is date of admission), the IABP and PCPS were removed (Figure 4) and prednisolone was tapered over a period of 8 weeks.

The patient has been doing well without any cardiac events since discharge and echocardiographic findings have remained normal during follow-up of 6 months (Figure 2B).

Anti-IgG to T. canis was detected in his serum by a commercial multiple-dot ELISA kit (SRL, Tokyo, Japan), although we could not find evidence of the parasites in the myocardial biopsy. Therefore, we performed further examination at the Department of Parasitology, Miyazaki Medical University, Miyazaki, Japan. Binding of patient serum to parasite antigens was tested using ELISA. Briefly, wells of microtiter plates were coated with 10 μg/ml of T. canis larval excretory–secretory antigen, and incubated with diluted samples (1:900–1:2,700). Binding of antibodies to T. canis antigen was detected with horse-radish peroxidase-conjugated anti human IgG and optical densities were read with a microplate reader (BioRAD). The patient had eaten raw deer meat 1 week before admission, so the final diagnosis was fulminant eosinophilic myocarditis caused by a hypersensitivity reaction to VLM after T. canis infection. We got the result 4 months after he had been discharged and prescribed albendazole (600 mg/day), which was continued for 4 weeks without any adverse effect.

Discussion

Acute fulminant eosinophilic myocarditis is a rare disorder of unknown etiology, frequently resulting in cardiogenic shock and a fatal clinical course. Predisposing factors include viral infection, history of allergic diathesis, and initiation of new medications[6] It has been suggested[7] that there are 3 clinical stages of eosinophilic myocarditis: acute necrotizing phase, thrombotic phase and endomyocardial fibrosis phase. Loffler's endomyocarditis is considered to correspond to the second stage of eosinophilic endomyocardial disease. The third stage probably corresponds to restrictive myocarditis. Differential diagnoses include other types of myocarditis, Churg-Strauss syndrome, hypersensitivity reaction, malignant diseases, parasitic infection or hypereosinophilic syndrome. Eosinophilic myocarditis associated with hypereosinophilic syndrome is usually less acute and less severe than acute fulminant necrotizing eosinophilic myocarditis[8] In the present case, the pathological findings were compatible with fulminant necrotizing eosinophilic myocarditis.

Because the symptoms of the patient appeared after eating raw deer meat and because the antibody titer against T. canis was high, we made a final diagnosis of eosinophilic myocarditis associated with VLM because of T. canis infection. T. canis, the common dog roundworm, is 1 of the causative agents of VLM. When embryonated eggs of T. canis from contaminated meat reach the human gastrointestinal tract, they hatch and enter the portal system, reaching the liver. Some larvae then migrate to the lungs and heart through the systemic circulation[9,10] A previous case of myocarditis associated with VLM has been reported[11] and another in Japan[12] so the present case is a very rare occurrence. Although the Myocarditis Treatment Trial found no statistical advantage of corticosteroid treatment in biopsy-proven myocarditis (Dallas Criteria)[2] it has been suggested that eosinophilic heart disease may be a subset with greater responsiveness[1] to corticosteroids. However, acute fulminant eosinophilic myocarditis is usually fatal and antemortem diagnosis is difficult. Corticosteroid therapy in the early stage can have favorable effect if early diagnosis by endomyocardial biopsy is made. In the present case, endomyocardial biopsy in the acute phase was helpful for diagnosis and therapeutic decision-making. Necrotizing eosinophilic myocarditis associated with VLM is very rare, but it should be taken into consideration.

Albendazole is a benzimidazole anthelmintic and is used as treatment for various parasitic infections. The mechanism of its anthelmintic action is inhibition of tubulin polymerization and microtubule-dependent glucose uptake inhibition. It has been reported that the incidence of adverse effects of albendazole is 23% and that the main adverse effect is liver injury (16%)[13] We were able to continue albendazole treatment of the present patient for 4 weeks without any adverse effects. Prompt anthelmintic treatment for parasite infection is recommended in eosinophilic myocarditis associated with VLM, so we should have administered albendazole earlier in the clinical course.

The patient was thought to be complicated by cardiac tamponade on admission, so PCPS was immediately inserted because of rapid worsening of left ventricular contraction and cardiogenic shock. The patient became hemodynamically stable with the PCPS and pericardial effusion decreased dramatically after starting corticosteroid therapy, so we did not perform pericardiocentesis on admission, which we probably should have done.

References

1. Jones SR, Herskowitz A, Hutchins GM, Bauqhman KL. Effects of immunosuppressive therapy in biopsy-proved myocarditis and borderline myocarditis on left ventricular function. Am J Cardiol 1991;

68: 370–376.
2. Mason JW, O'Connell JB, Herskowitz A, Rose NR, McManus BM, Billinqham ME, et al. A clinical trial of immunosuppressive therapy for myocarditis: The Myocarditis Treatment Trial Investigators. N Engl J Med 1995; 333: 269–275.
3. Beaver PC, Snyder CH, Carrera GM, Dent JH, Lafferty JW. Chronic eosinophilia due to visceral larva migrans: Report of three cases. Pediatrics 1952; 9: 7–19.
4. Dent JH, Nichols RL, Beaver PC, Carrera GM, Staggers RJ. Visceral larva migrans with a case report. Am J Pathol 1956; 32: 777–803.
5. Cookston M, Stober M, Kayes SG. Eosinophilic myocarditis in CBA/J mice infected with Toxocara canis. Am J Pathol 1990; 136: 1137–1145.
6. Watanabe N, Nakagawa S, Fukunaga T, Fukuoka S, Hatakeyama K, Hayashi T. Acute necrotizing eosinophilic myocarditis successfully treated by high dose methylprednisolone. Jpn Circ J 2001; 65: 923–926.
7. Brockington IF, Olsen EG. Eosinophilia and endomyocardial fibrosis. Postgrad Med J 1972; 48: 740–741.
8. Cooper LT, Zehr KJ. Biventricular assist device placement and immunosuppression as therapy for necrotizing eosinophilic myocarditis. Nat Clin Pract Cardiovasc Med 2005; 2: 544–548.
9. Mok CH. Visceral larva migrans: A discussion based on review of the literature. Clin Pediatr (Phil) 1968; 7: 565–573.
10. Woodruff AW. Toxocariasis. BMJ 1970; 3: 663–669.
11. Vargo TA, Singer DB, Gillatte PC, Fernbach DJ. Myocarditis due to visceral larva migrans. J Pediatr 1977; 90: 322–323.
12. Abe K, Shimokawa H, Kubota T, Nawa Y, Takeshita A. Myocarditis associated with visceral larva migrans due to Toxocara canis. Intern Med 2002; 41: 706–708.
13. Drugs in Japan Forum. Drugs in Japan 2007; 209–210.

RESEARCH LETTER

Identification of new inhibitors for alternative NADH dehydrogenase (NDH-II)

Tatsushi Mogi[1], Kazunobu Matsushita[2], Yoshiro Murase[3], Kenji Kawahara[1], Hideto Miyoshi[4], Hideaki Ui[5], Kazuro Shiomi[5], Satoshi Ōmura[5] & Kiyoshi Kita[1]

[1]Department of Biomedical Chemistry, Graduate School of Medicine, The University of Tokyo, Tokyo, Japan; [2]Department of Biological Chemistry, Faculty of Agriculture, Yamaguchi University, Yamaguchi, Japan; [3]Mycobacterium Reference Center, The Research Institute of Tuberculosis, Antituberculosis Association, Tokyo, Japan; [4]Division of Applied Life Sciences, Graduate School of Agriculture, Kyoto University, Kyoto, Japan; and [5]Kitasato Institute for Life Sciences and Graduate School of Infection Control Sciences, Kitasato University, Tokyo, Japan

Correspondence: Tatsushi Mogi, Department of Biomedical Chemistry, Graduate School of Medicine, The University of Tokyo, Bunkyo-ku, Tokyo 113-0033, Japan. Tel.: +81 3 5841 8202; fax: +81 3 5841 3444; e-mail: tmogi@m.u-tokyo.ac.jp

Received 7 October 2008; accepted 6 November 2008.
First published online 8 December 2008.

DOI:10.1111/j.1574-6968.2008.01451.x

Editor: Atsushi Yokota

Keywords
acetic acid bacteria; respiratory chain; NADH dehydrogenase; inhibitor; antibiotics.

Abstract

In bacterial membranes and plant, fungus and protist mitochondria, NADH dehydrogenase (NDH-II) serves as an alternative NADH : quinone reductase, a non-proton-pumping single-subunit enzyme bound to the membrane surface. Because NDH-II is absent in mammalian mitochondria, it is a promising target for new antibiotics. However, inhibitors for NDH-II are rare and unspecific. Taking advantage of the simple organization of the respiratory chain in *Gluconobacter oxydans*, we carried out screening of natural compounds and identified scopafungin and gramicidin S as inhibitors for *G. oxydans* NDH-II. Further, we examined their effects on *Mycobacterium smegmatis* and *Plasmodium yoelii* NDH-II as model pathogen enzymes.

Introduction

Obligate aerobe *Gluconobacter* is a genus of acetic acid bacteria that can oxidize a broad range of sugars, sugar alcohols and sugar acids. Low biomass yield and the rapid and incomplete oxidation of carbon sources (oxidative fermentation), which take place in the periplasm and is accompanied by the accumulation of products into the culture medium, make them suitable for industrial applications for bioconversion to obtain a variety of valuable products (Deppenmeier *et al.*, 2002; Adachi *et al.*, 2007). Key oxidation processes are catalyzed by dehydrogenases bound to the outer surface of the cytoplasmic membrane, and linked to the generation of proton-motive force (Matsushita *et al.*, 1994).

The recently released complete genome of *Gluconobacter oxydans* American Type Culture Collection 621H indicates that the respiratory chain lacks Complex I (NADH : quinone reductase, NDH-I), Complex II (succinate : quinone reductase) and Complex IV (cytochrome *c* oxidase) (Prust *et al.*, 2005). Genes encoding putative Complex III (quinol : cytochrome *c* reductase) and cytochrome *c* have been identified, but their functions are unclear because of the absence of cytochrome *c* oxidase. NADH produced in the cytoplasm is reoxidized by a single-subunit NADH dehydrogenase (NDH-II), a key enzyme for the regeneration of an oxidized form of NAD. NDH-II is bound peripherally to the inner surface of the cytoplasmic membrane and does not pump proton. Quinols generated by membrane-bound dehydrogenases are directly oxidized by cytochrome bo_3 oxidase (Matsushita *et al.*, 1987) and/or cyanide-insensitive oxidase (Ameyama *et al.*, 1987).

Taking advantage of the simple organization of the *Gluconobacter* respiratory chain (Matsushita *et al.*, 1994), here, we identified new inhibitors for NDH-II, which has been shown to be crucial for the adaptation of *Mycobacterium tuberculosis* (Shi *et al.*, 2005) and malaria parasite *Plasmodium* spp. (Fisher *et al.*, 2007) to host environments. From the screening of natural antibiotics in the Kitasato Institute for Life Sciences Chemical Library (Ui *et al.*, 2007),

we found the inhibitory activity of 36-membered ring macrolide scopafungin (Johnson & Dietz, 1971) and cyclic decapeptide gramicidin S (GS) (Izumiya *et al.*, 1979) (Fig. 1) for the *G. oxydans* NDH-II, and we examined their inhibitory mechanism and effects on *Mycobacterium smegmatis* and *Plasmodium yoelii* NDH-II.

Materials and methods

Preparation of bacterial membrane vesicles

Gluconobacter oxydans NBRC3172 (formerly *G. suboxydans* IFO12528) was grown aerobically in complex media containing 20 g of sodium D-gluconate, 5 g of D-glucose, 3 g of glycerol, 3 g of yeast extract and 2 g of polypepton (Nihon Pharmaceutical Co.) per 1 L using a 50-L jar fermentor at 30 °C. Cells were harvested at the late-log phase, suspended in 10 mM potassium phosphate (pH 6.0) and disrupted with a Rannie high-pressure laboratory homogenizer (model Mini-Lab, type 8.30H, Wilimington, MA). After centrifugation, to remove intact cells, the supernatant was centrifuged at 86 000 *g* for 60 min and precipitated membranes were suspended in 50 mM Tris-HCl (pH 7.4) containing 10% sucrose and 3 mM EDTA. *Mycobacterium smegmatis* mc^2155 was grown aerobically at 37 °C, and membrane vesicles were prepared from the stationary-phase cells (Kana *et al.*, 2001).

Preparation of malaria parasite mitochondria

Rodent malaria *P. yoelii* strain 17XL was injected intraperitoneally into 8-week-old female BALB/c mice, and parasite mitochondria were prepared as in Takashima *et al.* (2001). Rat liver mitochondria were prepared as in Johnson & Lardy (1967).

Enzyme assay

NADH : ubiquinone-1 (Q_1) reductase (NQR) activity of the membranes was measured at 25 °C in 100 mM Tris-HCl (pH 7.4) containing 10% sucrose, 0.02% Tween 20 (Calbiochem), 10 mM KCN and 100 μM Q_1 with a V-660 double monochromatic spectrophotometer (JASCO, Tokyo, Japan) (Mogi *et al.*, 2008), and reactions were initiated by addition of NADH ($\varepsilon_{340} = 6.3\ mM^{-1}\ cm^{-1}$, Roche) at a final concentration of 200 μM. Mitochondrial NQR and succinate : Q_1 reductase activities were determined in 50 mM potassium phosphate (pH 7.4) containing 1 mM $MgCl_2$, 0.02% Tween 20, 2 mM KCN and 100 μM Q_1 ($\varepsilon_{275} = 12.3\ mM^{-1}\ cm^{-1}$), and reactions were initiated by 200 μM NADH or 10 mM potassium succinate, respectively. NADH oxidase activity was measured in the absence of Q_1. Data analysis was carried out as in Mogi *et al.* (2008).

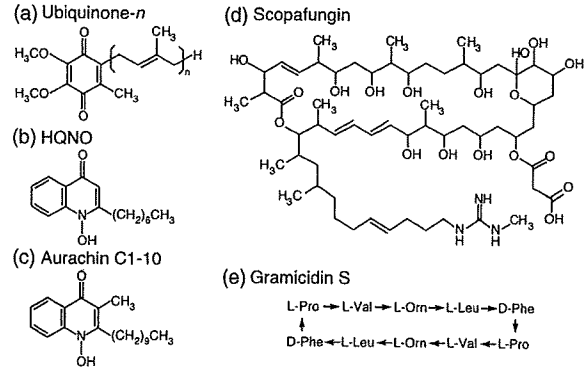

Fig. 1. Structures of ubiquinone, HQNO, aurachin C1–10, scopafungin and GS.

Materials

Synthesis of aurachin C 1-10 (Miyoshi *et al.*, 1999) was carried out as described previously. 2-Heptyl-4-hydroxyquinoline-*N*-oxide (HQNO) was obtained from Sigma.

Results and discussion

Screening of Kitasato Institute for Life Sciences Chemical Library

From the screening of a total of 304 microbial compounds (Ui *et al.*, 2007) at final concentrations of 5 $\mu g\ mL^{-1}$ with *G. oxydans* membranes, we revealed the inhibitory activities of scopafungin (niphimycin; residual activity, 33%), GS (31%), polymixin B (51%), aculeacin A (63%), funiculosin (68%) and staurosporine (70%) on 0.2 mM NADH–0.1 mM Q_1 reductase activity of NDH-II.

Inhibitors for NDH-II are rare and mostly unspecific (Kerscher, 2000). Recently, quinolone derivatives [1-hydroxy-2-dodecyl-4(1*H*)quinolone, HQNO and aurachin C] were identified as potent inhibitors for the quinone reduction site of yeast NDH-II (Eschemann *et al.*, 2005; Yamashita *et al.*, 2007). We examined the effects of quinolone inhibitors on the *G. oxydans* NDH-II and found that HQNO and aurachin C 1-10 at 10 μM reduced the NQR activity of the *G. oxydans* membranes to 28% and 12%, respectively, of the control level. Because of the limitation in the availability of isolated natural compounds, we examined further effects of scopafungin and GS (Fig. 1), which are not structurally related to ubiquinone, but showed potent inhibitory activities on the *G. oxydans* NDH-II.

Determination of 50% inhibitory concentration (IC_{50}) values for NDH-II inhibitors

We examined the dependence of the NQR activity on the concentration of GS, scopafungin, HQNO and aurachin C 1-10 and determined their IC_{50} to be 1.2 ± 0.2, 6.2 ± 0.5,

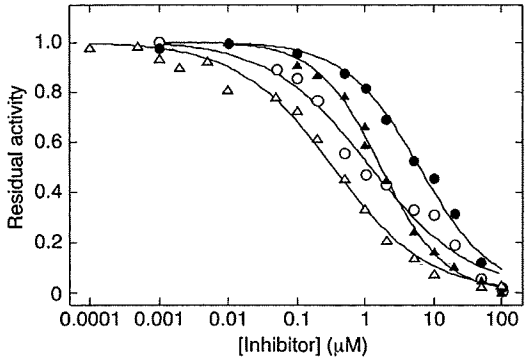

Fig. 2. Inhibition of *Gluconobacter oxydans* NDH-II by scopafungin, GS, HQNO and aurachin C 1-10. NQR activity of *G. oxydans* membranes (10 μg protein mL^{-1}) was determined in the presence of scopafungin (●), GS (○), HQNO (▲) or aurachin C1–10 (△). Data points were average values from duplicate assay. Control activity was 10.2 U mg^{-1} protein. IC_{50} values for GS, scopafungin, HQNO and aurachin C1–10 were estimated to be 1.2, 6.2, 1.7 and 0.34 μM, respectively.

1.7 ± 0.1 and 0.34 ± 0.04 μM, respectively (Fig. 2). The IC_{50} value for GS was < 3.5 μM for the *Escherichia coli bd*-type quinol oxidase (Mogi *et al.*, 2008), and the values for HQNO and aurachin C are comparable to 8 and 0.2 μM, respectively, of yeast *Saccharomyces cerevisiae* NDI1 (Yamashita *et al.*, 2007).

Kinetic analysis of inhibition of NADH-Q_1 reductase activity of NDH-II by scopafungin and GS

NADH-dependent NQR activity showed simple Michaelis–Menten kinetics with an apparent K_m value of 157 μM for NADH (at 0.2 mM Q_1) (Fig. 3). The K_m value for NADH was higher than those reported for yeast *Yarrowia lipolytica* NDE (15 μM) (Kerscher *et al.*, 1999), yeast *S. cerevisiae* NDI1 (31 μM) (de Vries & Grivell, 1988), human malaria *Plasmodium falciparum* NDH-II (17 μM) (Biagini *et al.*, 2006) and *E. coli* Ndh (34 μM) (Björklöf *et al.*, 2000). Q_1-dependent NQR activity followed Michaelis–Menten kinetics with an apparent K_m value of 16.2 ± 0.7 μM (Q_1) (Fig. 4), which is similar to 16 μM (Q_1) in *P. falciparum* (Biagini *et al.*, 2006), 5.9 μM (Q_1) in *E. coli* (Björklöf *et al.*, 2000), 6.4 μM (Q_2) in *M. tuberculosis* (Kana *et al.*, 2001) and 7 μM (decyl benzoquinone) in *Y. lipolytica* (Eschemann *et al.*, 2005).

Macrolide scopafungin and cyclic decapeptide GS (Fig. 1) are structurally unrelated to both NADH and ubiquinone, and serve as noncompetitive inhibitors ($K_i = 5.5$ and 1.4 μM, respectively) for the NADH-binding site of NDH-II (Fig. 3). Unexpectedly, scopafungin and GS were found to be a mixed-type inhibitor and a competitive inhibitor for the quinone-binding site, respectively (Fig. 4). These results

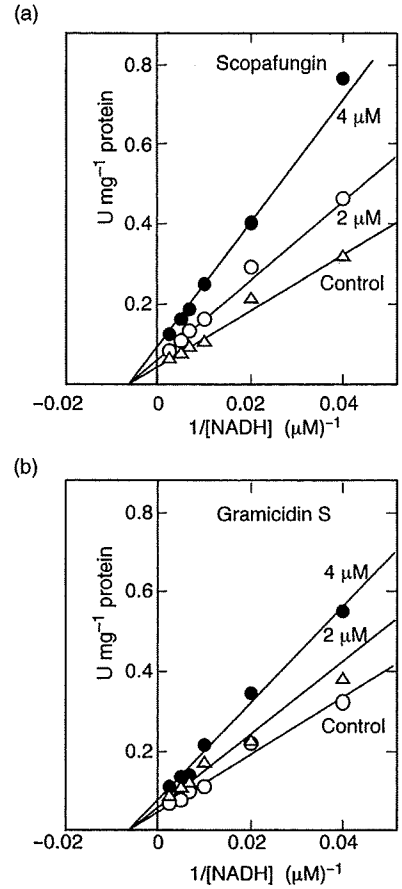

Fig. 3. Kinetic analysis of effects of scopafungin and GS on the NADH-dependent NQR activity of *Gluconobacter oxydans* NDH-II. (a) Noncompetitive inhibition by scopafungin. Apparent V_{max} values were estimated to be 19.3 (control), 17.2 (2 μM scopafungin) and 11.9 (4 μM scopafungin) U mg^{-1} protein at $K_m = 157$ μM. (b) Noncompetitive inhibition by GS. Apparent V_{max} values were determined to be 21.9 (control), 16.5 (2 μM GS) and 13.2 (4 μM GS) U mg^{-1} protein at $K_m = 157$ μM.

indicate that both compounds bind to a hydrophobic binding pocket on NDH-II molecule, which is closer to the quinone reduction site.

Effects of scopafungin and GS on *M. smegmatis* and *P. yoelii* NDH-II

Macrolide antibiotics are known to be more active against Gram-positive bacteria and fungi (Izumiya *et al.*, 1979), but targets remain to be determined while GS is active against Gram-positive and Gram-negative bacteria and several pathogenic fungi (Kondejewski *et al.*, 1996). The primary mode of the action of GS is generally assumed to perturb lipid packing, resulting in the destruction of the membrane integrity and enhancement of the permeability of the lipid bilayer (Prenner *et al.*, 1997). Very recently, we found that

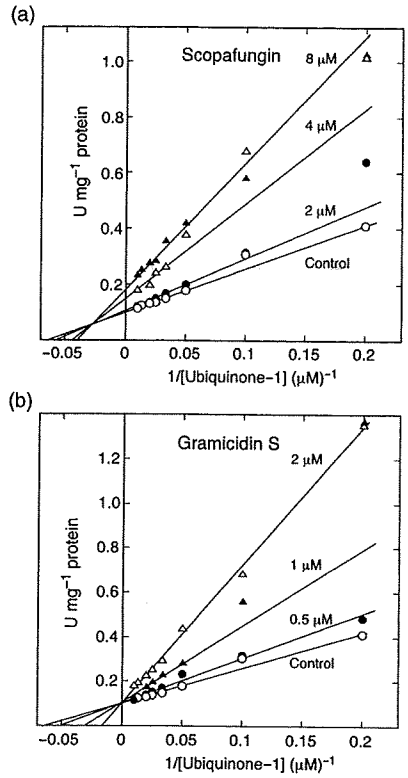

Fig. 4. Kinetic analysis of effects of scopafungin and GS on the Q_1-dependent NQR activity of *Gluconobacter oxydans* NDH-II. (a) Mixed-type inhibition by scopafungin. Apparent K_m (μM) and V_{max} (U mg^{-1} protein) values were estimated to be 15.5 and 9.6 (control), 17.4 and 9.0 (2 μM scopafungin), 22.4 and 6.5 (4 μM scopafungin) and 24.9 and 5.3 (8 μM scopafungin). (b) Competitive inhibition by GS. The apparent K_m values were determined to be 16.9 (control), 21.7 (0.5 μM GS), 37.5 (1 μM GS) and 68.3 (2 μM GS) μM at $V_{max} = 10.1$ U mg^{-1} protein.

GS can directly inhibit the *E. coli bd*-type quinol oxidase in a mixed-type manner (Mogi *et al.*, 2008). From the screening of the Kitasato Institute for Life Sciences Chemical Library with *G. oxydans* membranes, here, we identified scopafungin and GS as new inhibitors for NDH-II.

NDH-II is a promising target of new antibiotics because of the absence of NDH-II in mammalian mitochondria. The antiplasmodial activities of NDH-II inhibitors, HQNO ($IC_{50} = 3.5$ μM) (Fry *et al.*, 1990) and 1-hydroxy-2-dodecyl-4(1H) quinolone ($IC_{50} = 14$ nM) (Saleh *et al.*, 2007), have been reported previously. Thus, we examined the effects of scopafungin and GS on the NQR activity of *M. smegmatis* and rodent malaria *P. yoelii* NDH-II. At 10 μM, scopafungin showed minor effects on rat liver mitochondrial Complex I, Complex II and Complex III *plus* IV, while GS reduced NADH oxidase activity to 35% of the control by inhibiting the Complex III *plus* IV activity (Table 1). Although the IC_{50} values of scopafungin and GS for rodent malaria NDH-II were rather high (16.1 ± 3.0 and 23.0 ± 7.1 μM, respectively), both scopafungin and GS inhibited *M. smegmatis* NDH-II with IC_{50} values of 9.8 ± 0.7 and 2.0 ± 0.1 μM, respectively (Fig. 5), which are better than 12 μM of trifluoperazine for *M. tuberculosis* NDH-II (Yano *et al.*, 2006). Because scopafungin did not show severe effects on mammalian respiratory enzymes, it is a candidate for antimycobacterial agents. Here, we showed that the Kitasato Institute for Life Sciences Chemical Library (Ui *et al.*, 2007) was a powerful source for new potent antibiotics targeting to respiratory enzymes. For the identification of potential candidates, screening with recombinant NDH-IIs is currently underway in our laboratory.

Table 1. Effects of GS and scopafungin on the rat liver mitochondrial respiratory enzymes

	Relative residual activity (%)	
Enzyme activity	10 μM GS	10 μM scopafungin
NADH : Q_1 reductase (Complex I)	107	89
Succinate : Q_1 reductase (Complex II)	90	82
NADH oxidase (Complexes I+III+IV)	35	84

Control activities were 154 (NADH : Q_1 reductase), 247 (succinate : Q_1 reductase) and 102 (NADH oxidase) mU mg^{-1} protein.

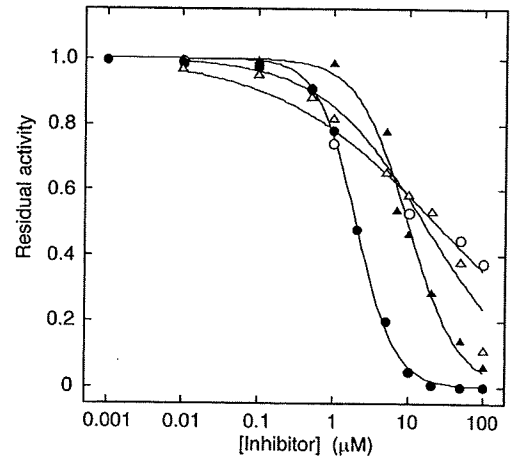

Fig. 5. Inhibition of *Mycobacterium smegmatis* and *Plasmodium yoelii* NDH-II by GS and scopafungin. Control activities of *M. smegmatis* membranes and *P. yoelii* mitochondria were 1.1 and 0.071 U mg^{-1} protein, respectively. The IC_{50} values for GS were estimated to be 2.0 (*M. smegmatis*, ●) and 23 (*P. yoelii*, ○) μM and those for scopafungin were 9.8 (*M. smegmatis*, ▲) and 16 (*P. yoelii*, △) μM.

Acknowledgements

This study was supported by a grant-in-aid for scientific research (20570124 to T.M.), scientific research on Priority Areas (18073004 to K.K.) and Creative Scientific Research (18GS0314 to K.K.) from the Japanese Ministry of Education, Science, Culture, Sports, and Technology.